

# Analysis of Specific Absorption Rate and Current Density in an Energy Transmission System for a Wireless Capsule Endoscope

Kenji Shiba, *Member, IEEE*, Tomohiro Nagato, Toshio Tsuji, *Member, IEEE* and Kohji Koshiji *Member, IEEE*.

**Abstract**—This paper reports on the electromagnetic influences on the analysis of biological tissue surrounding a prototype energy transmission system for a wireless capsule endoscope. Specific absorption rate (SAR) and current density were analyzed by electromagnetic simulator in a model consisting of primary coil and a human trunk including the skin, fat, muscle, small intestine, blood and backbone. SAR and current density as a function of frequency and output power were analyzed. The SAR was below the basic restrictions of the International Commission on Non-Ionizing Radiation Protection (ICNIRP). At the same time, the results for current density show that the influence on biological tissue was lowest in the 300-400 kHz range, indicating that it was possible to transmit energy safely up to 100 mW.

## I. INTRODUCTION

Recently, much progress has been made in the development of a wireless capsule endoscope for taking video images of digestive organs [1]-[6]. Currently, M2A [1] (Given Imaging) and Endo Capsule (Olympus) [2] are commercially available systems for this purpose in the world. However, this system is unable to take video pictures or inspect in detail all of a gastrointestinal organ, because of the time restraints for filming (8 hours, 2 frames per second) imposed by operating with internal batteries. Thus, methods for supplying energy from outside the body to a capsule endoscope have been proposed to extend the operating time of the capsule endoscope. One of these methods involves transmitting energy using electromagnetic induction between two coils, respectively placed inside and outside the body [7]-[10]. However, to make this method practical, we must investigate the electromagnetic influence of an energy transmission system on biological tissue.

Electromagnetic influences on biological tissue include thermal effects and stimulant action. The former is the effect of generating Joule heat on biological tissue, and the latter involves exciting neurons and muscles by the induced current. The Specific Absorption Rate (SAR, W/kg) is often used as an index of the thermal effects, and current density, A/m<sup>2</sup>, is often used as an index of the stimulant action. The guidelines for SAR and current density are provided by the International Commission in Non-Ionizing Radiation

Protection (ICNIRP) [11] for the frequency range of 100 kHz-10 MHz.

In this paper, we analyze the previously unknown SAR and current density in biological tissue surrounding the energy transmission system for the capsule endoscope. To determine the proper transmission conditions (frequency and output power) to reduce electromagnetic influences on biological tissue, we analyze the localized SAR (average value of biological tissue 10 g) and current density on the biological tissue surrounding a primary coil for transmitting power by an electromagnetic simulator using TLM method [12]-[13].

## II. METHODS

### A. Energy Transmission System

A wireless capsule endoscope with an energy transmission system consists of an image transmitter, image sensor, LEDs and receiver coil. According to recent papers, these devices require a power input of about 15 mW-0.9 W [1],[10].

Fig. 1(a) shows a typical circuit of the energy transmission system. In this circuit,  $\omega$ ,  $V_1$ ,  $V_2$ ,  $I_1$ ,  $I_2$ ,  $r_1$ ,  $r_2$ ,  $R_L$  and  $M$  show, respectively, the angular frequency, input and output voltage, input and output current, primary and secondary coil's resistance, load for the capsule endoscope and mutual inductance. Voltage from the power supply was transmitted to the secondary side via primary coil, and supplied to the load  $R_L$ .

In past research, 100-700 kHz was used for the transmission frequency. For example, we determined that an output power of 0.9 W was obtained when AC voltage was applied at a frequency of 500 kHz [9]. Therefore, in the present study, we calculated SAR and current density as a function of frequency 100-700 kHz, with the above-mentioned coils (of Fig. 1(b)). There were 14 turns of the primary coil ( $L_1=100$  mH, square), and approximately 150 turns of the secondary coil, which was wound around a ferrite-core ( $L_2=470$  mH,  $\phi 5$  mm  $\times$  18 mm). These coils were decided with consideration for the input current and transmitting efficiency.

### B. Specific Absorption Rate and Current Density

Generally, SAR is expressed by Equation (1):

$$\text{SAR} = \frac{\sigma E^2}{\rho} \quad (1)$$

where  $\sigma$  is the electric conductivity of the biological tissue (S/m),  $E$  is the root mean square of the electric field (V/m), and  $\rho$  is the density of the biological tissue (kg/m<sup>3</sup>).

Manuscript received April 1, 2007. This work was supported in part by a Grant-in-Aid for Young Scientists (B) 17760234 in Japan Society for the Promotion of Science.

K. Shiba, T. Nagato, T. Tsuji are with Graduate School of Engineering, Hiroshima University, Higashi-Hiroshima, Hiroshima, Japan shiba@bsys.hiroshima-u.ac.jp

K. Koshiji is with Tokyo University of Science, Chiba, Japan koshiji@ee.noda.tus.ac.jp

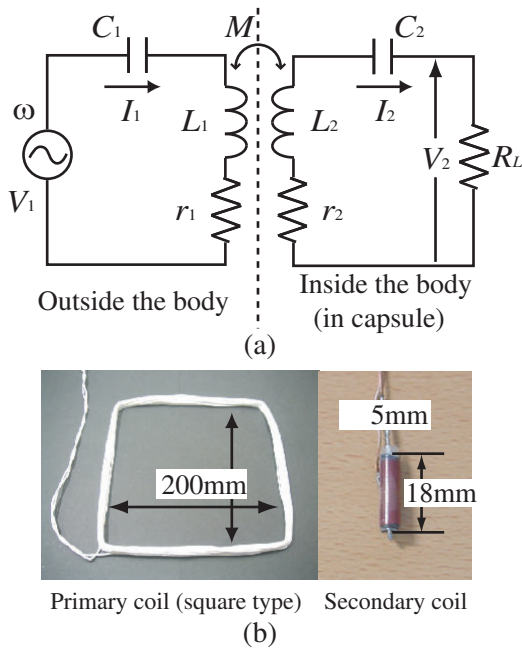


Fig. 1. (a) Equivalent circuit of the energy transmission system. (b) Coils for energy transmission.

TABLE I

BASIC RESTRICTIONS (IN OCCUPATIONAL EXPOSURE) FOR TIME VARYING ELECTRIC AND MAGNETIC FIELDS FOR FREQUENCIES 100KHZ-10MHZ (ICNIRP).

Current density for head and trunk (mA/m <sup>2</sup> ) (rms)	Localized SAR (head and trunk) (W/kg)
$f/100$	10

Current density  $J$  is expressed by Equation (2):

$$J = \pi R f \sigma \mu H \quad (2)$$

where  $R$  is the radius of the loop for induced current (m),  $\mu$  is the magnetic permeability (H/m) and  $H$  is the average value of the magnetic fields in the loop for induced current.

SAR and current density have basic restrictions (Table I) defined by ICNIRP. In this research, basic restrictions for occupational exposure were employed.

### C. Numerical analysis of the SAR and current density

1) *Transmission-Line Modeling method*: Micro-Stripes (Flomerics, Japan branch), an electromagnetic simulator employing the TLM method [12], was used for the analyses. TLM is based on an analogy between the electromagnetic field and the grid of transmission lines. A mathematical derivation of the TLM method can be directly obtained from a full wave time-domain solution to Maxwell's equations.

SAR is obtained from analysis, and current density  $J$  is calculated from the magnetic field obtained from analysis by Eq. (2). This paper also analyzes SAR as a localized SAR,

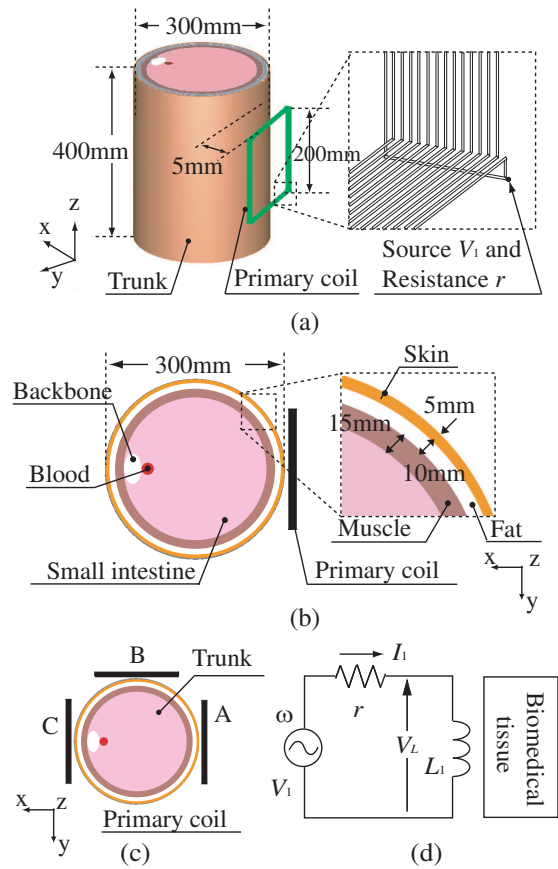


Fig. 2. (a), (b) Analytical model (human body's trunk). (c) Arrangement of primary coil. (d) Equivalent circuit for the analytical model.

which is represented as an average value of biological tissue 10 g.

2) *Biological model for numerical analysis*: Fig. 2 shows a biological model for numerical analysis. In Fig. 2(a), the trunk (abdominal part) of a human body is modeled as an elliptical cylinder with diameter 300 mm, and a primary coil (200 mm  $\times$  200 mm, 14 turns) is placed 5 mm away from the trunk. Fig. 2(b) shows a top view of the trunk model, which is composed of skin (thickness: 5 mm), fat (thickness: 10 mm), muscle (thickness: 15 mm), small intestine ( $\phi$  240 mm), blood ( $\phi$  20 mm) and backbone ( $\phi$  30 mm  $\times$  50 mm). The primary coil was arranged in A-C as shown in Fig. 2(c).

The biological tissue's electrical characteristics were based on IFAC (Institute for Applied Physics "Nello Carrara" [14]-[15]). In addition, an average value of 1000 kg/m<sup>3</sup> was used to represent the density of biological tissue consisting of skin, fat, muscle, small intestine, blood and backbone, and relative permeability was 1 [16].

3) *Circuit model for the numerical analysis*: The equivalent circuit of the analytical model is shown in Fig. 2(d). Input current  $I_1$  and the terminal voltage of coil  $V_L$  were adjusted by  $V_1$  and  $r$  to be equal to the actual measurement values in the prototype coils (when  $R_L=10$  W).

As an analysis condition, the frequency was varied between 100-700 kHz on output power of 0.01, 0.05, 0.1, 0.5 and 0.9 W.

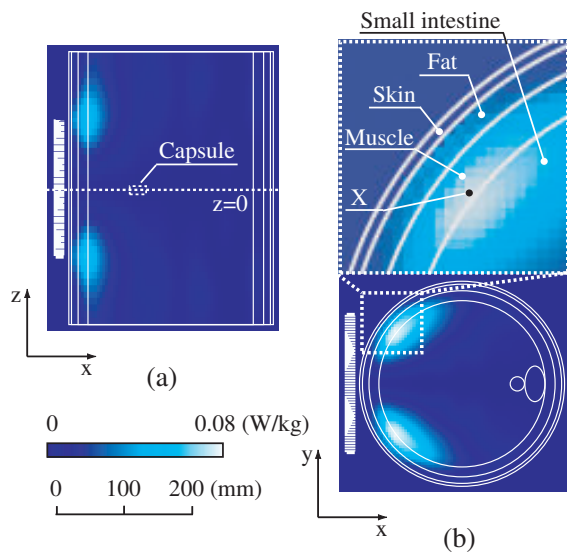


Fig. 3. The localized SAR distribution.

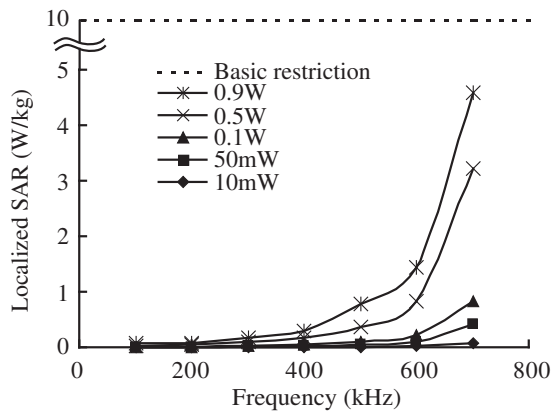


Fig. 4. The SAR as a function of frequency.

### III. RESULTS

#### A. Analysis of Localized SAR

At a frequency of 200 kHz and an output power of 0.1 W, the maximum SAR values for the arrangement of the primary coil (A-C) were A: 12.2 mW/kg, B: 12.1 mW/kg and C: 11.2 mW/kg, respectively. From these results, the maximum SAR value appears in arrangement A. Therefore, the results for arrangement A is shown here.

The SAR distributions for a frequency of 200 kHz and output power of 0.9 W are shown in Fig. 3. Fig. 3(a) is the SAR distribution of an x-z plane through the model's central axis, and Fig. 3(b) is one of an x-y plane at z=0. The results show that SAR was large on the inner side of the trunk's surface and was the maximum at point X, which is the part in boundary of muscle and small intestine, as muscle and small intestine are more conductive than skin and fat.

Next, Fig. 4 shows the analytical results of the localized SAR on point X as a function of frequency when the output power was varied. Here, the dotted line indicates ICNIRP's basic restrictions on exposure. The plot shows that for every value of output power it's possible to remain within the

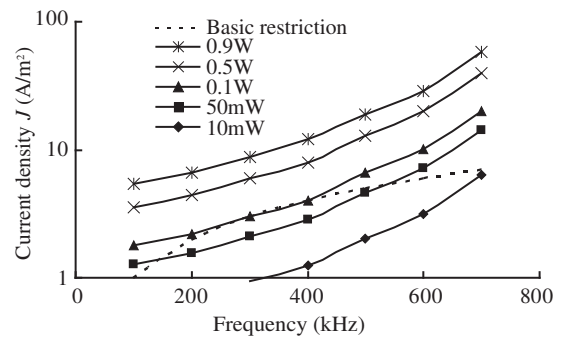


Fig. 5. The current density as a function of frequency.

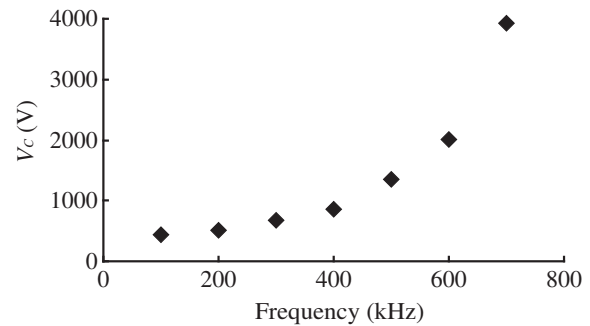


Fig. 6. The measurement results of the terminal voltage of the primary coil.

ICNIRP's basic restrictions.

#### B. Analysis of Current density

At a frequency of 200 kHz and output power of 0.1 W, the maximum value for current density for arrangement of the primary coil (A-C) was an equivalent value, A-C: 2.21 A/m<sup>2</sup>. Therefore, the results of the arrangement of A is shown here.

Fig. 5 shows the analytical results of the maximum current density as a function of frequency when the output power was varied. Here, the dotted line indicates ICNIRP's basic restrictions. The plot shows that influences on biological tissue become smallest at 300-400 kHz when compared with the ICNIRP's basic restrictions; thus, it is possible to transmit power up to a maximum of 100 mW.

### IV. DISCUSSION

The SAR and current density in biological tissue surrounding the primary coil were analyzed.

The SAR results show that SAR was maximized in the boundary of muscle and the small intestine, and it increased as frequency and output power increased. The results of SAR show that it is possible to remain within the ICNIRP's basic restrictions for every value of output power from 10 mW-0.9 W.

Fig. 6 shows the measurement results of the terminal voltage of the prototype primary coil with an output power of 0.9 W. A comparison of the plots in Fig. 4 with Fig. 6 shows that the SAR depended on the terminal voltage of the primary coil. Therefore, to reduce the SAR, it is necessary to reduce the terminal voltage of the primary coil.

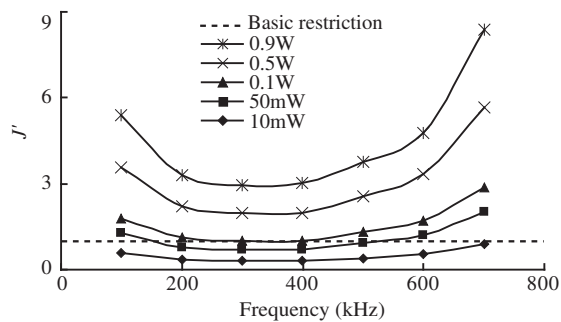


Fig. 7. The normalized current density  $J'$  as a function of frequency.

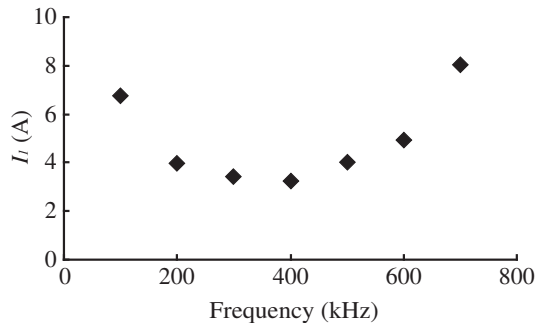


Fig. 8. The measurements of the primary coil's current.

In Fig. 5, the results of the current density show that current density increased as frequency and output power increased. Moreover, the influences on biological tissue become smallest at 300-400 kHz when compared with the ICNIRP's basic restrictions. Thus, it is possible to transmit power up to a maximum of 100 mW.

Next, Fig. 7 shows the normalized current density  $J'$ , which is divided by the ICNIRP's basic restrictions in Fig. 5. Fig. 7 shows that if  $J' \leq 1$ , the current density remains within the ICNIRP's basic restrictions. In addition, the measurement results of input current  $I_1$  with an output power of 0.9 W, are shown in Fig. 8. The plot in Fig. 7 corresponds with that in Fig. 8, suggesting that the current density depended on the current in the primary coil. Therefore, to transmit more power safely, it's necessary to reduce the current density by either reducing the primary coil's current.

## V. CONCLUSION

In this paper, we analyzed SAR and current density in the biological tissue surrounding a primary coil of an energy transmission system for a wireless capsule endoscope. In the results, the SAR remains within the ICNIRP's basic restrictions for every value of output power from 10 mW to 0.9 W at frequencies of 100-700 kHz, and the current density become smallest at 300-400 kHz; thus, it is possible to transmit power up to a maximum of 100 mW.

In the future, it will be necessary to design an energy transmission system considering safety and performance.

## VI. ACKNOWLEDGMENTS

The authors would like to thank Mr. Yasunobu Hasegawa and Ms. Natsumi Kuwano (Flomerics, Japan branch) for

their useful suggestions and assistance with regard to the electromagnetic simulator.

## REFERENCES

- [1] G. Iddan, G. Meron, A. Glukhovsky, and P. Swain, "Wireless capsule endoscopy," *Nature.*, vol. 405, p. 417, 2000.
- [2] Olympus Launches High-resolution Capsule Endoscope in Europe -The capsule endoscope system for small bowel which allows real time observation-. Olympus Corp. Tokyo, Japan. [Online]. Available: <http://www.olympus-global.com/en/news/2005b/nr051013capsle.cfm?chm=4>
- [3] D. G. Adler, and C. J. Gostout, "Wireless capsule endoscopy," *Hospital Physician.*, pp. 14-22, May. 2003.
- [4] X. Xie, G. L. Li, B. Y. Chi, X. Y. Yu, C. Zhang, and Z. H. Wang, "Micro-system design for wireless endoscopy system," in *Proc. IEEE, Engineering in Medicine and Biology 27th Annual Conference*, Shanghai, China, Sep. 2005, pp. 7135-7138.
- [5] ASGE Technology Status Evaluation Report: wireless capsule endoscopy. *Gastrointestinal Endoscopy.*, vol. 63, no. 4, pp. 539-549, 2006.
- [6] H. J. Park, J. C. Park, J. H. Lee, Y. K. Moon, B. S. Song, C. H. Won, H. C. Choi, J. T. Lee, and J. H. Cho, "New method of moving control for wireless endoscopic capsule using electrical stimulus," *IEICE transaction on fundamentals of electronics, communications and computer sciences.*, vol. E88-A, pp. 1476-1480, 2005.
- [7] B. Lenaerts, and R. Puers, "Inductive powering of a freely moving system," *Sensors and Actuators. A*, vol. 123-124, pp. 522-30, 2005.
- [8] S. W. Lee, J. D. Kim, J. H. Son, M. H. Ryo, and J. Kim, "Design of two-dimensional coils for wireless power transmission to in vivo robotic capsule," in *Proc. IEEE, Engineering in Medicine and Biology 27th Annual Conference*, Shanghai, China, Sep. 2005, pp. 6631-6634.
- [9] A. Morimasa, T. Nagato, K. Shiba, and T. Tsuji. "Energy transmission system for endoscopy capsule -an attempt to improve the transmission ability-," *Society of Life Support Technology 21th Annual Conference.*, Mie, Japan, Dec. 2005, p. 50.
- [10] K. Inagaki, and K. Koshiji, "Investigation of transcutaneous energy transmission system for a capsuled camera inside the body," *The 17th Symposium on Electromagnetics and Dynamics.*, Kochi, Japan, Jun. 2005, pp.22-24.
- [11] International Commission on Non-Ionizing Radiation Protection, "Guidelines for limiting exposure to time-varying electric, magnetic, and electromagnetic fields (up to 300 GHz)," *Health Phys.*, vol. 74, no. 4, pp. 494-522, 1998.
- [12] C. Christopoulos, *The transmission-line modeling method.* New York: IEEE Press, 1995.
- [13] P. B. Johns, "A symmetrical condensed node for the TLM method," *IEEE Trans. Microwave Theory Tech.*, vol. MTT-35, no. 4, pp. 370-377, 1987.
- [14] C. Gabriel, S. Gabriel, and E. Corthout, "The dielectric properties of biological tissues: I. Literature survey," *Phys. Med. Biol.*, vol. 41, pp. 2231-2249, 1996.
- [15] S. Gabriel, R. W. Lau, and C. Gabriel, "The dielectric properties of biological tissues: II. Measurements in the frequency range 10 Hz to 20 GHz," *Phys. Med. Biol.*, vol. 41, pp. 2251-2269, 1996.
- [16] Japan Society of Medical Electronics and Biological Engineering, *Handbook of clinical engineering.* Tokyo: Corona Publishers, 1984. p.113.